Physical modeling and analysis of P-wave attenuation anisotropy in transversely isotropic media

Yaping Zhu, Ilya Tsvankin, and Pawan Dewangan
Center for Wave Phenomena, Department of Geophysics, Colorado School of Mines, Golden, CO 80401

ABSTRACT
The amplitudes and frequency content of seismic waves propagating through anisotropic formations may be strongly distorted by directionally dependent attenuation. Here, we present physical-modeling measurements of the P-wave attenuation coefficient in a transversely isotropic phenolic sample.
Using the spectral-ratio method, we estimated the group (effective) attenuation coefficient of P-waves transmitted through the sample for a wide range of propagation angles (from 0° to 90°) with the symmetry axis. Correction for the difference between the group and phase angles was used to obtain the normalized phase attenuation coefficient $\mathcal{A}$ that was inverted for the Thomsen-style attenuation-anisotropy parameters ϵ_Q and δ_Q. Whereas the symmetry axes of the angle-dependent coefficient $\mathcal{A}$ and of the velocity function have close orientations, the magnitude of attenuation anisotropy far exceeds that of velocity anisotropy. The quality factor Q increases more than tenfold from the symmetry (slow) direction to the isotropy plane (fast direction).
The robustness of our results depends critically on several factors, such as the availability of an accurate anisotropic velocity model and the adequacy of the "homogeneous" concept of wave propagation. The methodology discussed here can be extended to field measurements of anisotropic attenuation needed for AVO (amplitude variation with offset) analysis and seismic fracture detection.

Key words: attenuation, attenuation anisotropy, transverse isotropy, physical modeling

1 INTRODUCTION

Most existing publications on seismic anisotropy are devoted to the influence of angular velocity variation on the traveltimes and amplitudes of seismic waves. It is likely, however, that anisotropic formations are also characterized by directionally dependent attenuation related to the internal structure of the rock matrix or the presence of aligned fractures.

Various issues related to the analytic treatment of attenuation in anisotropic media were addressed by Borcherdt and Wennerberg (1985), Krebes and Le (1994), Carcione (2001), Červený and Pšenčík (2004) and others. For example, the quality factor Q, widely used as a measure of attenuation in isotropic media (e.g., Johnston and Toksöz, 1981), can be replaced by a *matrix* $\mathbf{Q}$ that describes anisotropic attenuation. Each element Q_{ij} of the quality-factor matrix is defined as the ratio of the real and imaginary parts of the corresponding stiffness coefficient (Carcione, 2001). Zhu and Tsvankin (2004, 2005) showed that the angle-dependent attenuation coefficients in transversely isotropic (TI) media can be obtained in a relatively simple form by using Thomsen-style attenuation parameters ϵ_Q, δ_Q, and γ_Q derived from the anisotropic $\mathbf{Q}$-matrix.

Although experimental measurements of attenuation, both in the field and on rock samples, are relatively rare, they indicate that the magnitude of attenuation anisotropy can exceed that of velocity anisotropy (e.g., Tao and King, 1990; Arts and Rasolofosaon, 1992; Prasad and Nur, 2003). For example, according to the measurements of Hosten et al. (1987) for an orthorhom-

bic sample made of composite material, the quality factor for P-waves changes from $Q \approx 6$ in the vertical direction to $Q \approx 35$ in the horizontal direction. Hosten et al. (1987) also show that the symmetry of the attenuation coefficient closely follows that of velocity.

Here, we extend the spectral-ratio method to anisotropic media and apply it to P-wave transmission data acquired in a symmetry plane of a phenolic sample. Fitting the theoretical normalized attenuation coefficient $\mathcal{A}$ to the measurements for a wide range of propagation angles yields large absolute values of the Thomsen-style attenuation-anisotropy parameters $\epsilon_{_Q}$ and $\delta_{_Q}$. Although the experiment was performed for a synthetic material, the results are indicative of the high potential of attenuation-anisotropy analysis for field seismic data.

2 THEORETICAL BACKGROUND

2.1 P-wave attenuation in TI media

Propagation of plane P- and SV-waves in TI media with TI attenuation is described by the Christoffel equation (Carcione, 2001; Zhu and Tsvankin, 2004, 2005):

$$\begin{aligned}&(\,\tilde{c}_{11}\tilde{k}_1^2+\tilde{c}_{55}\tilde{k}_3^2-\rho\,\omega^2)(\tilde{c}_{55}\tilde{k}_1^2+\tilde{c}_{33}\tilde{k}_3^2-\rho\,\omega^2)\\ &-\,[\,(\tilde{c}_{13}+\tilde{c}_{55})\tilde{k}_1\tilde{k}_3]^2=0\,,\end{aligned}\qquad(1)$$

where ρ is the density, ω is the angular frequency, $\tilde{c}_{ij} = c_{ij} + ic^I_{ij}$ are the complex stiffness coefficients (the symbol " ˜ " denotes a complex quantity), and $\tilde{\mathbf{k}} = \mathbf{k} - i\mathbf{k}^I$ is the complex wave vector. Generally, the vectors $\mathbf{k}$ and $\mathbf{k}^I$ (the imaginary part $\mathbf{k}^I$ is sometimes called the *attenuation vector*) have different orientations, which means that the phase (slowness) direction does not coincide with the direction of maximum attenuation. In that case, wave propagation is usually called "inhomogeneous", and the angle between $\mathbf{k}$ and $\mathbf{k}^I$ is called the "inhomogeneity angle." Whereas the inhomogeneity angle represents a free parameter in plane-wave propagation, it is usually small for wavefields excited by point sources in weakly attenuative media.

As discussed in Carcione (2001) and Zhu and Tsvankin (2004, 2005), by solving the Christoffel equation (1) one obtains the (real) phase velocity $v = \dfrac{\omega}{k}$ and the normalized attenuation coefficient $\mathcal{A} = \dfrac{k^I}{k}$. The coefficient $\mathcal{A}$, which determines the rate of amplitude decay per wavelength, is expressed through the quality-factor matrix ($Q_{ij} \equiv \dfrac{c_{ij}}{c^I_{ij}}$) and the real parts c_{ij} of the stiffnesses $\tilde{c}_{ij}$. Even for relatively simple media in which both c_{ij} and c^I_{ij} have TI (hexagonal) symmetry, the attenuation coefficients of P- and SV-waves have a rather complicated form.

To facilitate the analytic description of TI attenuation, Zhu and Tsvankin (2004, 2005) developed a notation based on the same principle as the commonly used Thomsen (1986) parameters for velocity anisotropy. For P- and SV-waves, the set of Thomsen-style attenuation-anisotropy parameters includes two reference (isotropic) quantities $\mathcal{A}_{P0}$ and $\mathcal{A}_{S0}$ and the dimensionless coefficients $\epsilon_{_Q}$ and $\delta_{_Q}$ (Appendix A). The parameters $\mathcal{A}_{P0} \equiv 1/(2Q_{33})$ and $\mathcal{A}_{S0} \equiv 1/(2Q_{55})$ are the P- and S-wave attenuation coefficients (respectively) in the symmetry direction, while $\epsilon_{_Q}$ and $\delta_{_Q}$ control the angle variation of the attenuation coefficients between the symmetry axis and the isotropy plane. In the limit of small attenuation and weak anisotropy (for both velocity and attenuation), the P-wave attenuation coefficient can be significantly simplified by linearizing the solution of the Christoffel equation (1) in the anisotropy parameters (Zhu and Tsvankin, 2004, 2005):

$$\mathcal{A}_P = \mathcal{A}_{P0}\,(1+\delta_{_Q}\sin^2\theta\cos^2\theta+\epsilon_{_Q}\sin^4\theta)\,,\qquad(2)$$

where θ is the phase angle with the symmetry axis. Equation (2) is obtained under the assumption of "homogeneous" wave propagation ($\mathbf{k} \parallel \mathbf{k}^I$), which is sufficiently accurate for P-waves generated by a point source in a homogeneous, weakly attenuative, weakly anisotropic medium.

Equation (2) has exactly the same form as Thomsen's (1986) weak-anisotropy approximation for the P-wave phase velocity. The parameter $\delta_{_Q}$ is responsible for the attenuation coefficient in near-vertical directions, while $\epsilon_{_Q}$ controls $\mathcal{A}_P$ close to the horizontal plane. The definition of the parameter $\delta_{_Q}$, however, is more complicated than that of Thomsen's parameter δ and reflects the coupling between the attenuation and velocity anisotropy (Zhu and Tsvankin, 2004, 2005). If both $\epsilon_{_Q}$ and $\delta_{_Q}$ go to zero, the approximate coefficient $\mathcal{A}_P$ becomes isotropic (i.e., independent of angle).

2.2 Spectral-ratio method for anisotropic attenuation

The spectral-ratio method is often used to estimate the attenuation coefficient in both physical modeling and field surveys. For laboratory experiments, application of this method typically involves amplitude measurements made under identical conditions for the sample of interest and for a reference purely elastic (non-attenuative) sample.

The amplitude spectrum of an arrival recorded for the reference sample [denoted by the superscript "(0)"] can be written as

$$U^{(0)}(\omega) = S(\omega)\,G^{(0)}(\mathbf{x}^{(0)})\;e^{-\mathbf{k}^{(0)I}\cdot\mathbf{x}^{(0)}}\;e^{i(\omega t-\mathbf{k}^{(0)}\cdot\mathbf{x}^{(0)})}\,,\qquad(3)$$

where $\mathbf{x}$ is the vector connecting the source and receiver, $S(\omega)$ is the spectrum of the source pulse, and the factor $G(\mathbf{x})$ incorporates the radiation pattern of the source and the geometrical spreading along the raypath. Similarly, the spectral amplitude for the attenuative sample

(superscript "(1)") has the form

$$U^{(1)}(\omega) = S(\omega)\, G^{(1)}(\mathbf{x}^{(1)})\; e^{-\mathbf{k}^{(1)I}\cdot\mathbf{x}^{(1)}}\; e^{i(\omega t - \mathbf{k}^{(1)}\cdot\mathbf{x}^{(1)})}\,. \tag{4}$$

If the reference trace is acquired for a purely elastic medium with $\mathbf{k}^{(0)I} = 0$, the logarithm of the amplitude ratio becomes

$$\ln\left|\frac{U^{(1)}}{U^{(0)}}\right| = \ln\left(\frac{G^{(1)}}{G^{(0)}}\right) - \mathbf{k}^{(1)I}\cdot\mathbf{x}^{(1)}\,. \tag{5}$$

The frequency dependence of the ratio $G^{(1)}/G^{(0)}$ is usually considered to be negligible in certain frequency range. Then the slope of the function $\ln\left|\frac{U^{(1)}}{U^{(0)}}\right|$ in this frequency range yields the "local" value of the Q-factor in the direction $\mathbf{x}$. If this slope changes with frequency ω, then $k^{(1)I} = |\mathbf{k}^{(1)I}|$ is not a linear function of frequency ω, and the assumption of frequency-independent Q is not valid.

The normalized attenuation coefficient introduced above is given by

$$\mathcal{A} = \frac{k^I}{k} = \frac{k^{(1)I}}{\omega}v\,, \tag{6}$$

which is simply the slope of $k^{(1)I}$ in the frequency domain corrected by the source-receiver distance and scaled by the phase velocity in the direction $\mathbf{x}^{(1)}$.

In isotropic media with isotropic (angle-independent) attenuation, the group attenuation coefficient $k^I_G = |\mathbf{k}^I_G|$ measured along the raypath using the spectral-ratio method is the same as the phase (plane-wave) attenuation coefficient $k^I = |\mathbf{k}^I|$. For anisotropic media with anisotropic attenuation, however, these two coefficients are different. If wave propagation is homogeneous (i.e., the inhomogeneity angle is negligible), the group and phase attenuation coefficients are related by the equation $k^I_G = k^I\cos(\psi - \theta)$, where ψ and θ are the group and phase angles, respectively (Zhu and Tsvankin, 2004).

Here, we employ the following procedure of inverting P-wave attenuation measurements for the attenuation-anisotropy parameters. First, the logarithmic spectral ratio yields the amplitude decay factor in the group (ray) direction, $k^{(1)I}_G x^{(1)}$ [equation (5)]. Second, using the phase and group angles obtained from the known velocity parameters of the sample, we evaluate the phase attenuation coefficient k^I and normalize it by the corresponding real wavenumber k [equation (6)] to estimate the coefficient $\mathcal{A} = \dfrac{k^I}{k}$. Third, the measurements of $\mathcal{A}$ for a wide range of phase angles θ are inverted for the attenuation-anisotropy parameters ϵ_Q and δ_Q. Approximate values of the parameters ϵ_Q and δ_Q can be found in a straightforward way from the linearized equation (2). More accurate results, however, are obtained by nonlinear inversion based on the exact Christoffel equation (1).

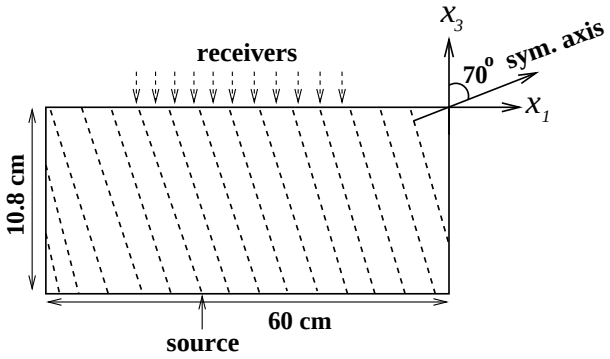

Figure 1. Physical model of a TI layer with the symmetry axis tilted at 70° (from Dewangan et al., 2005). The transmitted wavefield is excited by a transducer at the bottom of the model and recorded with a laser vibrometer.

Because of the coupling between attenuation and velocity anisotropy, estimation of the attenuation-anisotropy parameters requires knowledge of the anisotropic velocity field. Since the influence of attenuation on velocity is typically a second-order effect (Zhu and Tsvankin, 2005), anisotropic velocity analysis can be performed independently of attenuation measurements. Here, we use the results of Dewangan (2004) and Dewangan et al. (2005) who estimated the velocity-anisotropy parameters of our sample by inverting the reflection traveltimes of PP- and PS-waves.

3 EXPERIMENTAL SETUP

The goals of this experiment were to measure the directional dependence of the attenuation coefficient in a composite sample and to estimate the attenuation-anisotropy parameters. The material was XX-paper-based phenolic composed of thin layers of paper bonded with phenolic resin. This fine layering produces an effective anisotropic medium on the scale of the predominant wavelength. The sample was prepared by Dewangan (2004), who pasted phenolic blocks together at an angle, resulting in a transversely isotropic model with the symmetry axis tilted from the vertical by 70° (Figure 1).

Dewangan (2004) and Dewangan et al. (2005) show that the TTI model adequately explains the kinematics of multicomponent (P, S, and PS) data in the vertical measurement plane that contains the symmetry axis (the symmetry-axis plane). Although phenolic materials are generally known to be orthorhombic (e.g., Grechka et al., 1999), body-wave velocities and polarizations in the symmetry planes can be described by the corresponding TI equations (Tsvankin, 1997, 2001).

The original purpose of acquiring the transmission data used here (Figure 2a) was to verify the accuracy of the parameter-estimation results obtained by Dewan-

gan (2004) and Dewangan et al. (2005). The P-wave source transducer was fixed at the bottom of the model, and the wavefield was recorded with a laser vibrometer at the top of the model with a sampling interval of 2 mm in the same azimuth as that of the symmetry axis. The spread of the receiver locations was wide enough to record the full range of propagation angles (from 0° to 90°) with respect to the (tilted) symmetry axis.

For attenuation analysis we separated the first (direct) arrival by applying a Gaussian window to the raw data. The amplitude spectrum of the windowed first arrival, obtained by filtering out the low ($f < 5$ kHz) and high ($f > 750$ kHz) frequencies, is shown in Figure 2b. An aluminum block with negligibly small attenuation served as the reference model. The spectrum of the reference trace acquired by a receiver located directly above the source (Figure 3) was used to estimate the attenuation coefficient by means of the spectral-ratio method described above.

The parameters of the TTI velocity model needed to process the attenuation measurements were obtained by Dewangan et al. (2005) from reflection PP and PS data (Figure 4). Tilted transverse isotropy is described by the the P- and S-wave velocities in the symmetry direction (V_{P0} and V_{S0}, respectively), Thomsen anisotropy parameters ϵ and δ defined with respect to the symmetry axis, the angle ν between the symmetry axis and the vertical, and the thickness z of the sample. The known values of $\nu = 70°$ and $z = 10.8$ cm were accurately estimated from the reflection data, confirming that the velocity-inversion algorithm is robust.

4 MEASUREMENTS OF ATTENUATION ANISOTROPY

4.1 Estimation of the attenuation-anisotropy parameters

For each receiver position at the surface of the phenolic sample, we divided the spectrum of the recorded trace by that of the reference trace (Figure 3), as suggested by equation (5). Records with a low signal-to-noise ratio were excluded from the analysis. We use the frequency band of 60–110 kHz to estimate the attenuation coefficient. According to the spectral-ratio method described above, the relevant elements Q_{ij} of the quality-factor matrix are assumed to be constant in that frequency band.

The normalized phase-attenuation coefficient $\mathcal{A}$, obtained after correcting for the difference between group and phase attenuation (it does not exceed 6%), exhibits a pronounced variation between the slow (0°) and fast (90°) directions (Figure 5). The largest attenuation coefficient is observed along the symmetry axis ($\theta = 0°$), where the P-wave phase velocity reaches its minimum value. Since the symmetry direction is orthogonal to the multiple thin layers bonded together

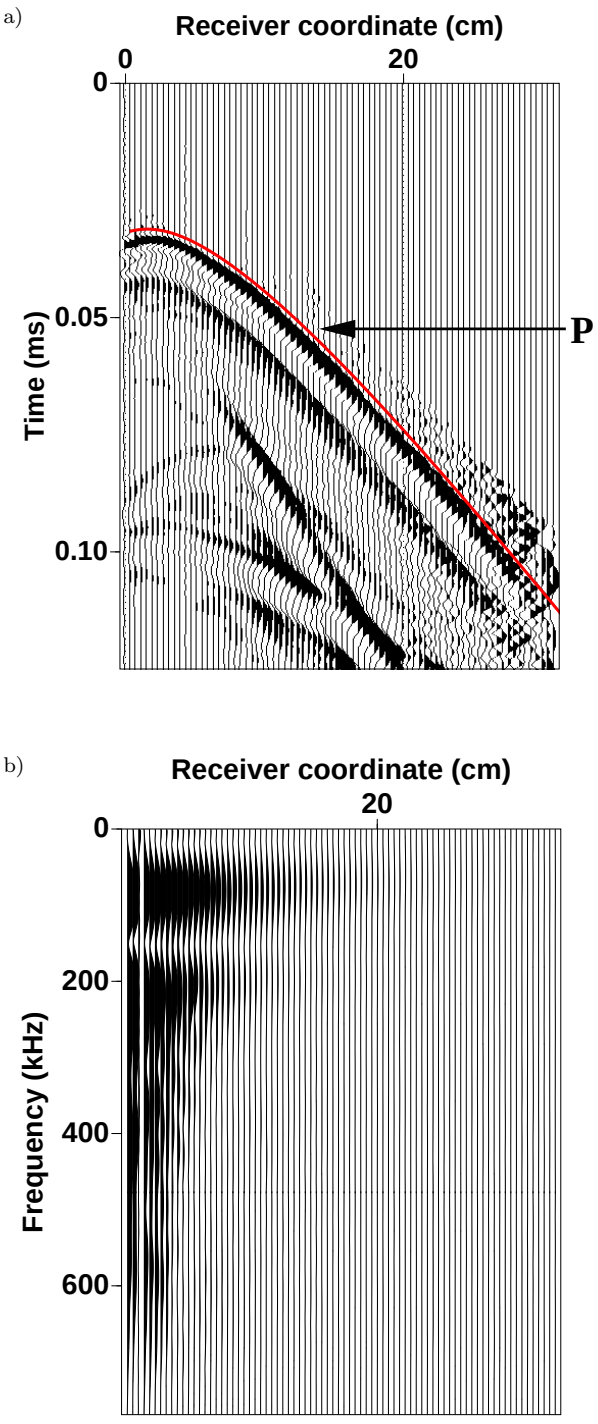

Figure 2. (a) Raw transmission data excited by a P-wave transducer, and (b) the amplitude spectrum of the windowed first arrival. The solid line is the P-wave traveltime modeled by Dewangan et al. (2005) using the inverted parameters from Figure 4. The time sampling interval is 2 μs, and the width of the Gaussian window is 40 samples.

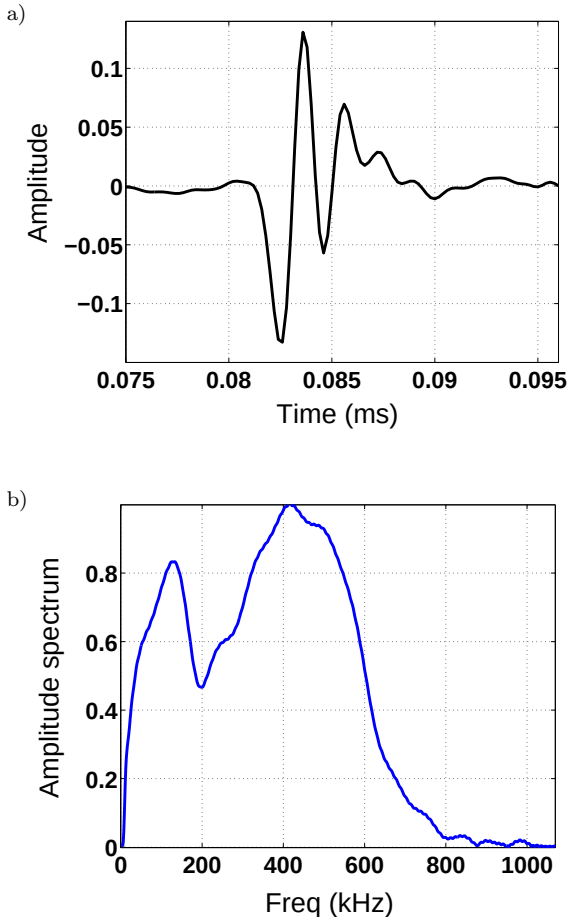

Figure 3. (a) Reference trace for vertical propagation through an aluminum block, and (b) its amplitude spectrum.

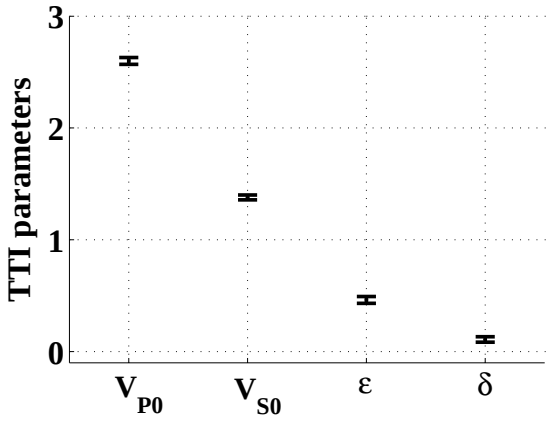

Figure 4. Parameters of the TTI model estimated from the reflection traveltimes of PP- and PS-waves in the symmetry-axis plane. The mean values are $V_{P0} = 2.6$ km/s, $V_{S0} = 1.38$ km/s, $\epsilon = 0.46$, and $\delta = 0.11$ (Dewangan et al., 2005). The error bars mark the standard deviations in each parameter obtained by applying the inversion algorithm to 200 realizations of input reflection traveltimes contaminated by Gaussian noise. The standard deviation of the noise times was equal to 1/8 of the dominant period of the reflection arrivals.

to form the model, the rapid increase in attenuation toward $\theta = 0^\circ$ is expected.

The polar plot of the attenuation coefficient, shown in Figure 6, indicates that the symmetry axis of the function $\mathcal{A}(\theta)$ is close to that for the velocity measurements. Although we did not acquire data for angles over 90° to reconstruct a more complete angle variation of $\mathcal{A}(\theta)$, the direction orthogonal to the layering should represent the symmetry axis for all physical properties of the model. To quantify the attenuation anisotropy, we used the Christoffel equation (1) to estimate the best-fit parameters: $\mathcal{A}_{P0} = 0.16$ ($Q_{33} = 3.2$), $\epsilon_{_Q} = -0.92$, and $\delta_{_Q} = -1.84$. The weak-attenuation, weak-anisotropy approximation (2) yields similar values ($\mathcal{A}_{P0} = 0.16$, $\epsilon_{_Q} = -0.86$, and $\delta_{_Q} = -1.91$) despite the large angular variation of $\mathcal{A}(\theta)$ (Figure 6).

While the fact that the largest attenuation coefficient for this model is observed at the velocity minimum is predictable, the extremely low value of $Q_{33} = 3.2$ is somewhat surprising. It should be mentioned, however, that estimates of the attenuation coefficient near the symmetry axis may be distorted by the relatively low reliability of amplitude measurements at long offsets corresponding to small angles θ (Figure 1). Problems in applying our methodology for large source-receiver distances may be related to such factors as the frequency-dependent geometrical spreading and the increased influenced of heterogeneity. In general, the spectral-ratio method may not be adequate for describing the frequency spectrum of the long-offset data.

An essential assumption behind the estimates of the attenuation-anisotropy parameters is that wave propagation through the model is homogeneous, and the inhomogeneity angle is negligibly small. Although the modeled attenuation coefficient provides a good fit to the measured curve, it is not clear how significant the inhomogeneity angle for this model may be and how it can influence the parameter-estimation results.

4.2 Uncertainty analysis

It is important to evaluate the uncertainty of the attenuation measurements caused by errors in the velocity-anisotropy parameters. Using the standard deviations in the parameters V_{P0}, ϵ, δ, and ν provided by Dewangan et al. (2005), we repeated our inversion procedure for 50 realizations of the input TTI velocity model (Figure 7). Although the variation of the estimated attenuation coefficients in some directions is substantial, the mean values of the attenuation-anisotropy parameters obtained from the best-fit curve $\mathcal{A}(\theta)$ are close to those listed above. The standard deviations are 2% for $\mathcal{A}_{P0}$, 0.01 for $\epsilon_{_Q}$, and 0.06 for $\delta_{_Q}$, which indicates that the

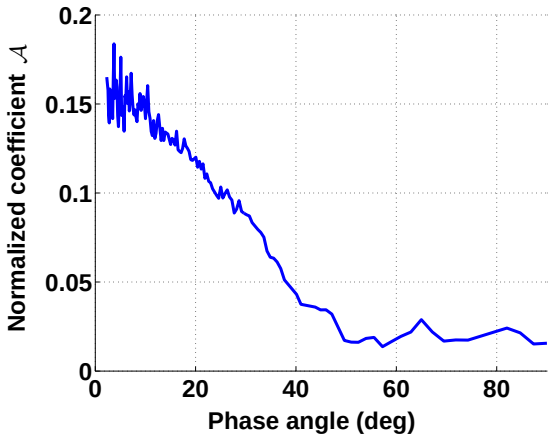

Figure 5. Measured normalized attenuation coefficient as a function of the phase angle.

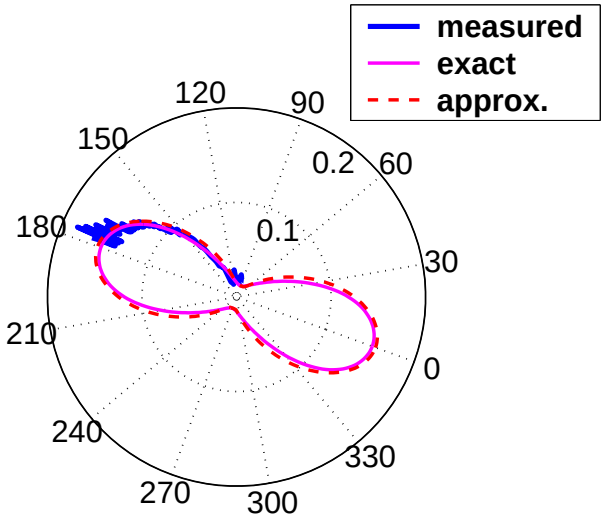

Figure 6. Attenuation measurements from Figure 5 (thick solid line) and the best-fit attenuation coefficients obtained using the Christoffel equation (1) (thin grey solid) and the approximation (2) (dashed).

influence of errors in the velocity field on our results is not significant.

Another potential source of uncertainty in the attenuation-anisotropy measurements is the choice of the frequency range used in the spectral-ratio method. Figure 8 shows the distribution of 50 realizations of the attenuation-anisotropy parameters obtained for variable upper and lower bounds of the frequency range. The means of the estimated parameters are $\mathcal{A}_{P0} = 0.16$ ($Q_{33} = 3.3$), $\epsilon_Q = -0.90$, and $\delta_Q = -1.94$, with the standard deviations equal to 3% for $\mathcal{A}_{P0}$, 0.06 for ϵ_Q, and 0.15 for δ_Q.

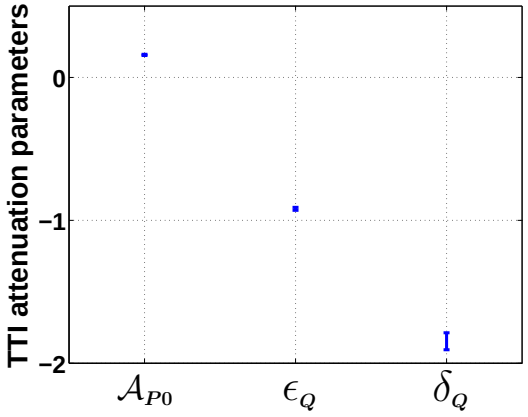

Figure 7. Influence of errors in the velocity model on the attenuation parameters. The error bars mark the standard deviations in each parameter obtained by applying our algorithm with 50 realizations of the input TTI velocity parameters. The standard deviations in the TTI parameters are taken from Dewangan et al. (2005).

The sensitivity of the attenuation-anisotropy parameters to moderate variations in the bounds of the frequency range is therefore not negligible. Note that since the parameter ϵ_Q for our model is close to -1, estimates of the normalized attenuation coefficient Q_{11} in the isotropy plane are unstable ($Q_{11} \to \infty$ when $\epsilon_Q \to -1$). Moderate variations of ϵ_Q within the errors bars in Figure 7 produce values of Q_{11} as low as 19.4 and as high as 93.5.

In accordance with the spectral-ratio method, we assume the quality-factor components Q_{ij} to be independent of frequency within the frequency range used for the analysis. The slope of the attenuation coefficient k^I in the frequency domain, however, is not constant, which implies that the attenuation-anisotropy parameters may vary with frequency.

A detailed analysis of the influence of noise in the data on attenuation estimates can be found in Vasconcelos and Jenner (2005).

5 DISCUSSION AND CONCLUSIONS

Since experimental measurements of attenuation are scarce, physical modeling of wave propagation through attenuative materials can provide useful insights into the magnitude and angular variation of the attenuation coefficient. Here, we applied the spectral-ratio method to P-waves transmitted through a transversely isotropic sample for a wide range of angles with the symmetry axis. After estimating the group (effective) attenuation along the raypath, we computed the corresponding phase (plane-wave) attenuation coefficient using a known TI velocity model. The difference between the phase and group attenuation, caused by the influence of velocity anisotropy, has to be accounted for in the

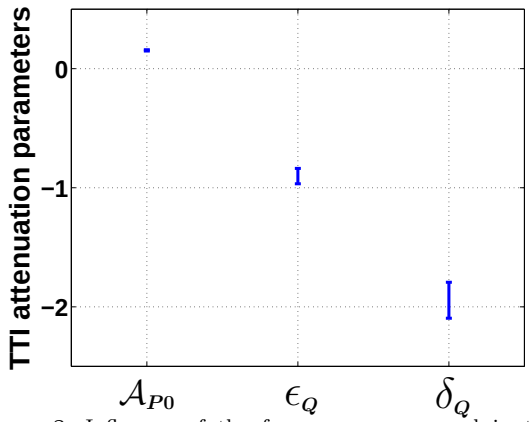

Figure 8. Influence of the frequency range used in the spectral-ratio method on the attenuation parameters. The error bars mark the standard deviations in each parameter obtained by applying our algorithm with 50 realizations of the upper and lower bounds of the frequency range. The upper bound was changed randomly between 88 kHz and 132 kHz, and the lower bound between 44 kHz and 66 kHz.

inversion of the attenuation coefficient for the medium parameters.

The reconstructed phase attenuation coefficient was normalized by the real wavenumber and used to estimate the Thomsen-style attenuation parameters $\mathcal{A}_{P0}$, ϵ_Q, and δ_Q introduced by Zhu and Tsvankin (2004, 2005). The large absolute values of both $\epsilon_Q = -0.92$ and $\delta_Q = -1.84$ reflect the high magnitude of the attenuation anisotropy, with the Q-factor increasing from 3.2 in the slow (symmetry-axis) direction to almost 40 in the fast (isotropy-plane) direction. This result corroborates the conclusions of some previous experimental studies (e.g., Hosten et al., 1987; Prasad and Nur, 2003) that attenuation is often more sensitive to anisotropy than is either phase velocity or reflection coefficient.

While the large difference between the attenuation coefficients in the two principal directions is unquestionable, the accuracy of our measurements strongly depends on several assumptions. First, the radiation pattern of the source and geometrical spreading are taken to be frequency-independent in the frequency range used in the spectral-ratio method. Since the sample is heterogeneous, it is desirable to test the validity of this assumption, particularly for relatively large source-receiver offsets. For example, the experiment can be redesigned by making measurements on two different-size samples of the same phenolic material. Then it would be possible to compute the spectral ratios for arrivals propagating in the same direction and recorded at different distances from the source. In this case, the potential frequency dependence of the radiation pattern would be removed from the attenuation measurement along with the spectrum of the source pulse, and no reference trace would be required.

Second, our analytic solutions for the attenuation coefficient are based on the common assumption of homogeneous wave propagation (i.e., the inhomogeneity angle is assumed to be negligible; see also Hosten et al., 1987). For strongly attenuative models with pronounced attenuation anisotropy, this assumption may cause errors in the interpretation of attenuation measurements. Also, if the model is layered, the inhomogeneity angle is governed by the boundary conditions and can be significant even for moderate values of the attenuation coefficients. Hence, future work should include investigations of the magnitude of the inhomogeneity angle and of its influence on the estimates of the attenuation-anisotropy parameters.

Third, our data-processing sequence did not include compensation for the possible contribution of attenuation to the coupling (i.e., reflection/transmission) coefficients at the source and receiver locations. In general, the attenuation-related frequency dependence of the reflection/transmission coefficients along the ray-path can cause distortions in the results of the spectral-ratio method.

Finally, since this work was restricted to compressional data, we were unable to evaluate the strength of the shear-wave attenuation anisotropy and estimate the full set of Thomsen-style anisotropy parameters (Zhu and Tsvankin, 2004, 2005). A more complete characterization of attenuation anisotropy requires combining P-waves with either shear data or converted (e.g., reflected) PS-waves.

6 ACKNOWLEDGMENTS

We are grateful to Kasper van Wijk and Mike Batzle of the Institute of Experimental Geophysics (IEG) at CSM for their help in data acquisition and to Ivan Vasconcelos, Mike Batzle, and Manika Prasad (all of CSM) for useful discussions. The support for this work was provided by the Consortium Project on Seismic Inverse Methods for Complex Structures at CWP and by the Chemical Sciences, Geosciences and Biosciences Division, Office of Basic Energy Sciences, U.S. Department of Energy.

REFERENCES

Arts, R. J., and Rasolofosaon P. N. J., 1992, Approximation of velocity and attenuation in general anisotropic rocks: 62nd Annual International Meeting, Society of Exploration Geophysicists, Expanded Abstracts, 640–643.

Borcherdt, R. D., and Wennerberg, L., 1985, General P, type-I S, and type-II S waves in anelastic solids; Inhomogeneous wave fields in low-loss solids: Bulletin of the Seismological Society of America, **75**, 1729–1763.

Carcione, J. M., 2001, Wave fields in real media: Wave propagation in anisotropic, anelastic, and porous media: Pergamon Press.

Červený, V., and Pšenčík, I., 2004, Plane waves in viscoelastic anisotropic media. Part 1: Theory: Preprint.

Dewangan, P., 2004, Processing and inversion of mode-converted waves using the PP+PS=SS method: PhD thesis, Center for Wave Phenomena, Colorado School of Mines.

Dewangan, P., Ts vankin, I., Batzle, M., van Wijk, K., and Haney, M., 2005, PS-wave moveout inversion for tilted transversely isotropic media: A physical-modeling study: CWP Project Review (this volume).

Grechka, V., Theophanis, S. and Tsvankin, I., 1999, Joint inversion of P- and PS-waves in orthorhombic media: Theory and a physical modeling study: Geophysics, **64**, 146–161.

Hosten, B., Deschamps, M., and Tittmann B. R., 1987, Inhomogeneous wave generation and propagation in lossy anisotropic solids: application to the characterization of viscoelastic composite materials: Journal of the Acoustical Society of America, **82**, 1763–1770.

Krebes, E. S., and Le, L. H. T., 1994, Inhomogeneous plane waves and cylindrical waves in anisotropic anelastic media: Journal of Geophysical Research, **99**, 23899–23919.

Prasad, M., and Nur, A., 2003, Velocity and attenuation anisotropy in reservoir rocks: 73rd Annual International Meeting, Society of Exploration Geophysicists, Expanded Abstracts, 1652-1655.

Tao, G., and King, M. S., 1990, Shear-wave velocity and Q anisotropy in rocks: A laboratory study: International Journal of Rock Mechanics and Mining Sciences and Geomechanics Abstracts, **27**, 353–361.

Thomsen, L., 1986, Weak elastic anisotropy: Geophysics, **51**, 1954–1966.

Tsvankin, I., 1997, Anisotropic parameters and P–wave velocity for orthorhombic media: Geophysics, **62**, 1292–1309.

Tsvankin, I., 2001, Seismic signatures and analysis of reflection data in anisotropic media: Elsevier.

Vasconcelos, I., and Jenner, E., 2005, Estimation of azimuthally varying attenuation from surface seismic data: CWP Project Review.

Zhu, Y., and Tsvankin, I., 2004, Plane-wave propagation and radiation patterns in attenuative TI media: 74th Ann. Internat. Mtg., Soc. Expl. Geophys., Expanded Abstracts, 139–142.

Zhu, Y., and Tsvankin, I., 2005, Plane-wave propagation in attenuative TI media: Geophysics, under review.

APPENDIX A: THOMSEN-STYLE PARAMETERS FOR ATTENUATIVE TI MEDIA

The attenuation coefficients in transversely isotropic (TI) media with TI attenuation can be conveniently described using the Thomsen-style notation of Zhu and Tsvankin (2004, 2005). Instead of the five relevant components Q_{ij} of the quality-factor matrix, they defined two "isotropic" reference quantities ($\mathcal{A}_{P0}$ and $\mathcal{A}_{S0}$) and three dimensionless parameters (ϵ_Q, δ_Q, and γ_Q) describing attenuation anisotropy.

The reference parameters $\mathcal{A}_{P0}$ and $\mathcal{A}_{S0}$ represent the P- and S-wave attenuation coefficients (respectively) in the symmetry direction:

$$\mathcal{A}_{P0} = \frac{1}{2Q_{33}}\,, \tag{A1}$$

$$\mathcal{A}_{S0} = \frac{1}{2Q_{55}}\,. \tag{A2}$$

The parameter ϵ_Q denotes the fractional difference between the P-wave attenuation coefficients in the isotropy plane and along the symmetry axis:

$$\epsilon_Q \equiv \frac{1/Q_{11} - 1/Q_{33}}{1/Q_{33}} = \frac{Q_{33} - Q_{11}}{Q_{11}}\,. \tag{A3}$$

The parameter δ_Q is expressed through the curvature of the P-wave attenuation coefficient in the symmetry direction and, therefore, governs the angle variation of P-wave attenuation near the symmetry axis:

$$\delta_Q \equiv \frac{\dfrac{Q_{33}-Q_{55}}{Q_{55}}c_{55}\dfrac{(c_{13}+c_{33})^2}{(c_{33}-c_{55})} + 2\dfrac{Q_{33}-Q_{13}}{Q_{13}}c_{13}(c_{13}+c_{55})}{c_{33}(c_{33}-c_{55})}\,. \tag{A4}$$

Note that the definition of δ_Q involves the real parts of the stiffnesses c_{ij} or the velocity-anisotropy parameters, which is indicative of the coupling between the attenuation coefficient and velocity anisotropy. The third anisotropic parameter, γ_Q, is responsible for the attenuation anisotropy of SH-waves.

The simplified P-wave attenuation coefficient in terms of the Thomsen-style parameters $\mathcal{A}_{P0}$, ϵ_Q, and δ_Q is given in the main text, equation (2).